C24

Numerical Analysis of The Thermal Performance of Photovoltaic Panel in Hot Weather Regions using PCM Materials

Khalil Khanafer, PhD **Ali Al-Masri, PhD** **Austin Abbasspour**

Ibrahim Deiab, PhD

ABSTRACT

The aim of this study is to investigate the practical application of a PCM cooling system and assess how its geometric and thermophysical parameters impact the thermal behavior and efficiency of PV cells. A numerical modeling approach using the finite element method is employed to predict how the PCM properties affect the cooling performance of the system and the power output of the solar module. The thermal analysis takes into consideration the nonlinearity and transient nature of the problem. The boundary conditions in a hot climate zone, where temperatures reach approximately 50 °C, include cyclic variations in solar irradiation and ambient temperature over time. Through optimization of the PCM design variables such as melting temperature, thermal conductivity, and thickness, the cell temperature can be reduced by approximately 20%. This optimization also leads to an increase of about 8% in efficiency and power output. These findings suggest that utilizing a passive cooling system based on PCM can effectively enhance the power output of a solar PV module. The developed integrated model provides insights into the thermal behavior of the PV module and facilitates the selection of an appropriate PCM for practical implementation.

INTRODUCTION

Due to their distinct thermal characteristics and potential uses in numerous industries, phase change materials (PCMs) have attracted a lot of attention in recent years. PCMs present a possible means of addressing the problems brought on by high operating temperatures, thermal control, and energy efficiency in the context of photovoltaic (PV) systems. During operation, photovoltaic systems frequently experience high temperatures that could affect their performance and lifespan. PV modules can degrade more quickly and experience power losses as a result of excessive heat accumulation. By efficiently absorbing and storing extra heat produced by PV panels, PCM materials provide an innovative option for thermal management. PCMs may absorb a significant amount of thermal energy while keeping a practically constant temperature during the phase transition process. This characteristic enables PCMs to function as a thermal buffer, reducing temperature spikes and supplying PV

Khalil Khanafer is an assstant professor in the Department of Mechanical Engineering at University of Michigan, Accredited State University. **Ali Al-Masri** is a research fellow at Australian University – Kuwait, **Austin Abbasspour** is a student in the Mechanical Engineering at University of Michigan. **Ibrahim Deiab** is a professor in the Mechanical Engineering at University of Guelph.

modules with a constant operating environment [1-5]. Khanafer and Al-Masri (2022) utilized numerical analysis to examine the effectiveness of phase change materials (PCMs) in regulating and optimizing energy transfer within buildings. Using ANSYS software, they performed an optimization analysis to determine a specific combination of PCM thermophysical and geometrical parameters that would minimize heat flow into the building. The simulation spanned a period of 10 days, and the results demonstrated an impressive 80% reduction in the amount of heat entering the building when PCMs were employed. Shakibi et al. (2022) proposed a new configuration to enhance the thermal management system of photovoltaic (PV) panels, by incorporating a metal foam layer along with a phase change material (PCM). The arrangement allows for efficient dissipation of heat from the system during the energy-absorbing mode, leading to the cooling of PV panels. Numerical simulations and analysis were conducted to investigate the effects of foam-layer material, PCM thickness, and foam porosity. The results indicated that increasing the thickness of the PCM layer resulted in lower temperatures on the PV surface. The extracted curves demonstrated that lower porosity led to higher maximum PV temperature. Additionally, the average electrical efficiency for models with porosities of 0.9, 0.8, 0.4, and no foam were found to be 13.805%, 13.794%, 13.761%, and 13.714% respectively. Browne et al. (2015) conducted a comprehensive review of various methods employed for thermal management in photovoltaic modules. It was observed that regulating the temperature of PV systems containing crystalline silicon cells was the most economically viable approach when utilizing PV/PCM systems. This is due to the fact that temperature increases have a more significant negative impact on the efficiency of silicon solar cells compared to organic or thin film cells. Research studies have demonstrated that the incorporation of PCM contributes to the enhancement of PV system performance. However, further exploration and improvement are still required, particularly regarding the solidification and discharge processes of PCM.

For the effective utilization of PCM cooling systems, careful selection of its characteristics is crucial. These characteristics typically encompass thermophysical material properties and layer thickness. The melting temperature of the PCM, in particular, is a critical factor directly associated with the initiation of the latent heat absorption and release process, which is dependent on the temperature evolution within the system. Consequently, the suitable PCM material is primarily determined by the thermal boundary and operating conditions specific to the proposed PV system. Additionally, considerations related to economic and environmental aspects should also be taken into account during the decision-making process (Zarma et al, 2019). Numerous studies in the existing literature have explored the influence of PCM thermo-physical characteristics on the thermal performance of such systems, emphasizing the significance of appropriate material selection. Parameters such as melting point, latent heat, and thermal conductivity hold importance in this regard. Ultimately, the appropriate material choice is determined by the specific boundary and operating conditions of the system (Shaito et al., 2021).

This work aims to utilize computational modeling techniques to identify and optimize the design parameters of PCM systems. The focus is on developing thermal models that ensure the efficient utilization of PV module cooling systems in specific climatic zones. The numerical model employed incorporates a comprehensive analysis of transient heat transfer within the PV module and integrated PCM system. The investigation explores the impact of the thermophysical properties of the PCM, including their temperature-dependent variations, as well as the geometric characteristics that define the PCM layer. The thermal model that has been developed is seamlessly integrated with design exploration tools, employing response surface methodologies, design of experiments methodology, and optimization analysis. This integrated model is utilized to examine the influence of input parameters on the system response, which is characterized by the temperature, efficiency, and electric power output of the PV cell. Furthermore, optimization analysis is employed to determine the combination of input variables that minimizes the PV cell temperature, thereby optimizing the performance of the solar PV module and maximizing the efficient utilization of the PCM.

MATHEMATICAL FORMULATION

The solar panel being studied comprises a solar PV unit positioned on top of an aluminum box that contains PCM. The system's structure is depicted and explained using layers in Figure 2. The module design for this study is based on the information presented by Khatib and Elmenreich (2016). Assuming a cell size of 1 m², it is considered that heat losses through the sides of the PCM box are negligible when compared to the front and back surfaces. The geometric and thermophysical properties of the various components of the model are provided in Tables 1 and 2, respectively (Smith et al., 2014).

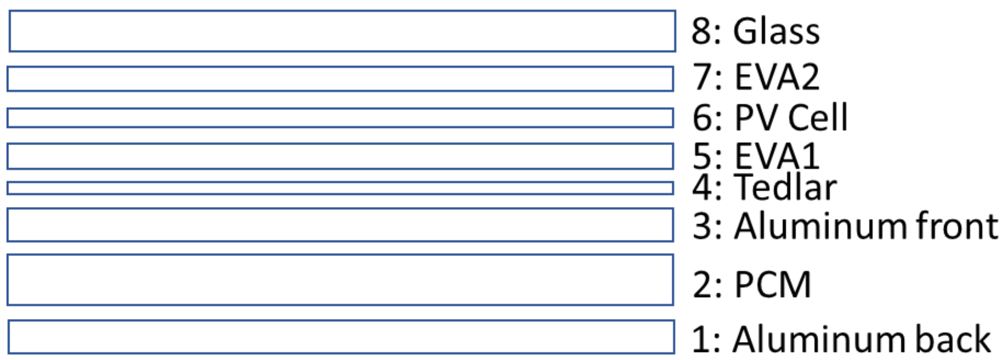

Figure 1. Structure of the PV solar panel.

Table 1. Parameters of the thermal model (Smith et al., 2014)

Layer	ρ [kg/m³]	c [J/(kg K)]	k [W/(m K)]	δ [mm]
Glass	3000	500	1.8	3
EVA	960	2090	0.35	0.5
PV cells	2330	677	148	0.225
Tedlar	1200	1250	0.2	0.1
Aluminum	2700	900	237	2

Table 2. Parameters of the PCM (n-Eicosene paraffin wax) thermal model (Smith et al., 2014)

Parameter	Value
ρ_s [kg/m³]	860
ρ_l [kg/m³]	780
c_s [J/(kg K)]	2900
c_l [J/(kg K)]	2100
Δh [kJ/kg]	210
k_s [W/(m K)]	0.24
k_l [W/(m K)]	0.15
T_m [°C]	20-60

The temperature variation in various solid layers is governed by the following heat conduction equation:

$$\rho c \frac{\partial T}{\partial t} = \nabla \bullet \left(k \nabla T \right) + s \qquad (1)$$

In Equation (1), the final term denoted as s represents the heat source per unit volume, which is specifically relevant in the domain of solar cells due to electric power generation. The thermophysical properties of materials typically vary with temperature and spatial coordinates. The specific material properties of the PCM investigated in this study can be found in

Table 2. In the context of a one-dimensional scenario, the temporal and spatial aspects are described as follows:

$$0 \le t \le t_f \tag{2}$$

$$0 \le y \le l \tag{3}$$

where l is the region thickness and t_f is the final time. In this case the energy equation given in Eq. (1) reduces to

$$\rho c \frac{\partial T}{\partial t} = \frac{\partial}{\partial y}\left(k \frac{\partial T}{\partial y}\right) + s \tag{4}$$

To examine the phase transition mechanism of the PCM, this study adopts an enthalpy formulation. Specifically, the specific enthalpy, denoted as h, is calculated using the following equation:

$$h = \int_{T_{ref}}^{T} \rho c dT \Leftrightarrow \frac{dh}{dT} = \rho c \tag{5}$$

T_{ref} is the reference temperature. Thus, the heat conduction equation in the PCM layer can be written as (Alizadeh et al., 2018):

$$\frac{\partial h}{\partial t} = \frac{\partial}{\partial y}\left(k \frac{\partial T}{\partial y}\right) \tag{6}$$

The relationship between the specific enthalpy and temperature is described by the following:

- In the interval $T < T_s$

$$h(T) = \int_{T_{ref}}^{T} \rho c_s dT \quad T < T_s \tag{7}$$

- In the interval $T_s \le T \le T_l$

$$h(T) = \int_{T_{ref}}^{T_s} \rho c_s dT + \int_{T_s}^{T} \left(\left(\frac{d(\Delta h)}{dT}\right) + \rho c_f\right) dT \tag{8}$$

- In the interval $T > T_l$

$$h(T) = \int_{T_{ref}}^{T_s} \rho c_s dT + \Delta h + \int_{T_s}^{T_l} \rho c_f dT + \int_{T_l}^{T} \rho c_l dT \tag{9}$$

Δh is the specific latent heat and the indices s and l designate the solidus and liquidus states of the material. The details of this method are well documented in the literature. The numerical solution to the problem is obtained using the finite element method, which has been extensively discussed and documented in existing literature.

Boundary and initial conditions

The initial condition is described by a constant temperature in the form:

$$T(y, t = 0) = T_i \tag{10}$$

which is set to 35°C in the entire computational domain. The solar panel's upper or frontal surface experiences solar irradiance, along with radiation and convection heat exchange with the surrounding environment. This phenomenon can be mathematically described using the following equations:

$$-k_g \left.\frac{\partial T}{\partial y}\right|_g = q_{irrad} + q_{rad,f} + q_{c,f} \tag{11}$$

$$q_{irrad} = \alpha_g G_\beta \tag{12}$$

$$q_{rad,f} = \sigma\left(\frac{1 + \cos(\beta)}{2}\right)\left(\varepsilon_{sky} T_a^4 - \varepsilon_g T_g^4\right) \tag{13}$$

$$q_{c,f} = h_c\left(T_a - T_g\right) \tag{14}$$

$$h_c = 1.247\left[\left(T_g - T_a\right) cos(\beta)\right]^{\frac{1}{3}} + 2.658\text{v} \tag{15}$$

The heat transfer coefficient, hc, takes into account both natural and forced convection and is influenced by temperature, wind speed (v), and tilt angle (β). On the other hand, the lower side of the solar panel experiences radiation and convection heat exchange with the surroundings, which can be represented by the following equations:

$$-k_{al}\left.\frac{\partial T}{\partial y}\right|_{al} = q_{rad,b} + q_{c,b} \tag{16}$$

$$q_{rad,b} = \sigma\left(\frac{1-\cos(\beta)}{2}\right)\left(\varepsilon_{ground}T_a^4 - \varepsilon_{al}T_{al}^4\right) \tag{17}$$

$$q_{c,b} = h_c\left(T_a - T_{al}\right) \tag{18}$$

Table 3 provides a comprehensive list of the parameters used in the thermal radiation model. To capture the anticipated variation in ambient temperature, a cyclic time function is employed, representing a range of 35°C to 49°C. This function is fitted to data obtained from temperature recordings in a hot region during the summer (Alqallaf and Alawadhi, 2013). The extreme temperatures experienced have a substantial influence on the thermal efficiency and performance of the solar PV system. In Figure 2, the hourly temperature fluctuations over a 24-hour period are presented alongside the solar irradiance curve, which is calculated based on Eq. (1).

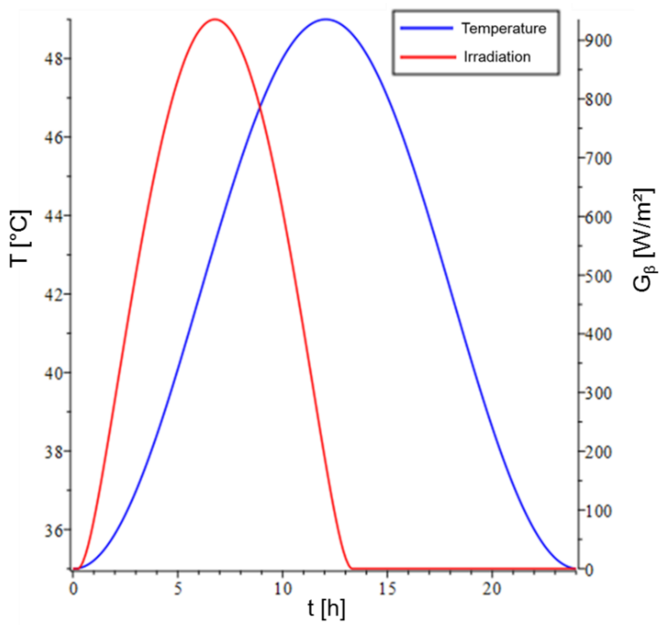

Figure 2. Hourly variation of ambient temperature and solar irradiance

The solar irradiance transmitted to the silicon cell, G_τ, is given by:

$$G_\tau = \alpha_{cell}\tau_g\left(1-\alpha_g\right)G_\beta \tag{19}$$

τ_g and α_g are the transitivity and absorptivity, respectively. Moreover, the generated electric power density is evaluated according to the mathematical model:

$$p_{el} = \frac{\eta A G_\beta}{V} \tag{20}$$

The symbols A and V denote the area of the glass surface and the volume of the cell unit, respectively. The module efficiency, represented by η, is determined by the characteristics of the cell and its dependence on temperature. This relationship allows for the calculation of module efficiency.

$$\eta = \eta_{ref}\left[1-\gamma\left(T_{cell}-25°C\right)\right] \quad (21)$$

With the reference efficiency evaluated at 25°C and 1000 W/m² and the decline in cell efficiency with respect to temperature are given by:

$$\eta_{ref} = 0.17, \quad \gamma = 4.5e-3K^{-1} \quad (22)$$

T_{cell} is the time dependent silicon cell temperature, and the other parameters are listed in Table 3.

Table 3. Solar panel parameters

Parameter	Value
A [m²]	1
α_{gl}	0.05
α_{cll}	0.9
τ_{gl}	0.95
σ [W/(m²K⁴)]	5.67e-8
ε_{gl}	0.95
ε_{al}	0.02
ε_{g}	0.95

Model Validation

The present numerical method was validated against the work of Huang et al. (2004). Figure 2 illustrates a comparison of the temporal variation of the temperature at the front surface of the aluminium plate between present and the results by Huang et al. (2004) when exposed to insolation of 1000 W/m2 and ambient temperature of 20 °C. A very good correlation between the results obtained by the presented model and the published data (Huang et al., 2004) as shownin Fig. 3.

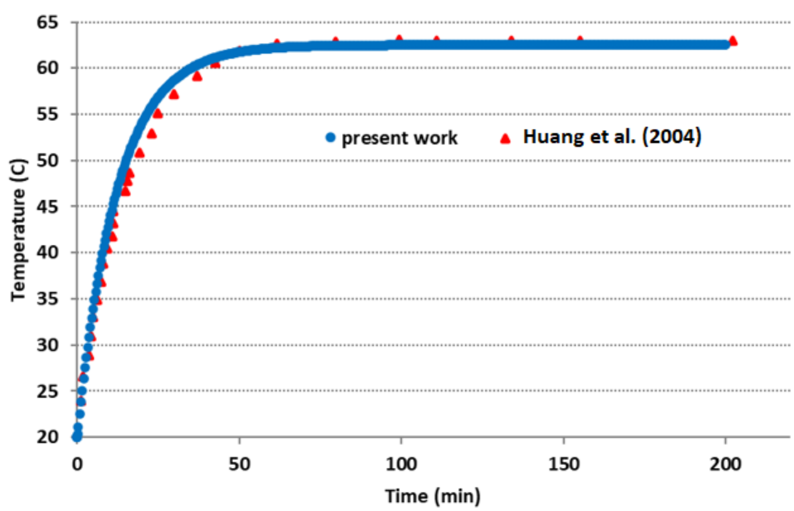

Figure 3. Comparison of the temporal variation of the temperature at the front surface of the aluminium plate between the present results and that of Huang et al. (2004).

RESULTS AND DISCUSSION

To analyze the thermal performance of the solar PV panel, a reference case study is conducted, excluding the PCM layer. The simulation covers a duration of 33 days. The analysis results, depicted in Figure 4, illustrate the temporal evolution of the temperature at various locations: the glass surface (Tgl), silicon cell (Tcell), and bottom aluminum surface (Tal), along with the ambient temperature.

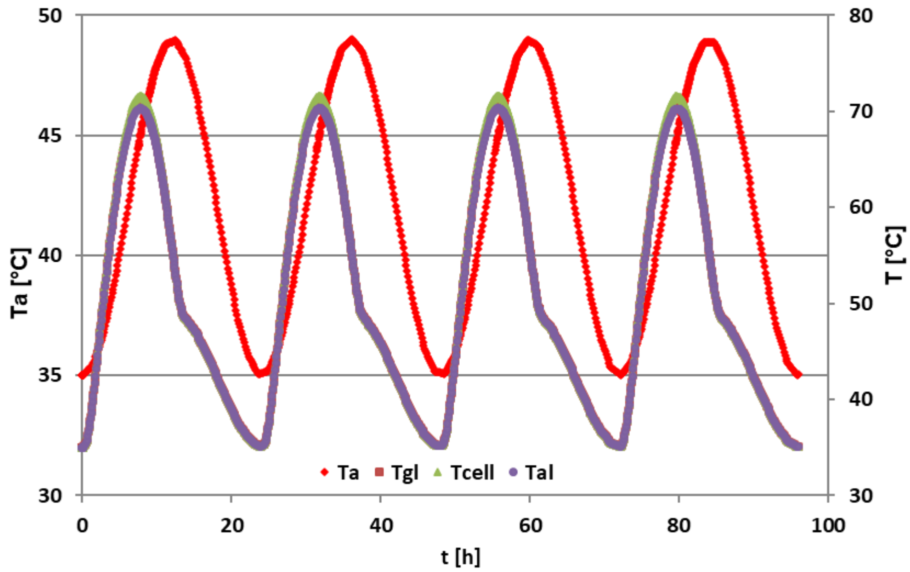

Figure 4. Temperature evolution in the solar panel layers.

The temperature curves exhibit similarities, indicating a negligible variation in the solar panel's temperature. This can be attributed to the low thermal resistances of the individual layers. The initial peak temperature of the panel reaches approximately 72°C, occurring approximately 7.8 hours after the start of the process. The first peak of the ambient temperature is observed to be shifted by approximately 4.7 hours. By analyzing the time history of the cell temperature, it becomes possible to assess the temporal variation in cell efficiency using Eq. (21). The resulting curve is presented in Figure 5. Due to temperature dependency, the efficiency fluctuates between an initial maximum value of 0.162 and a minimum value of 0.134, which is reached 7.8 hours into the process.

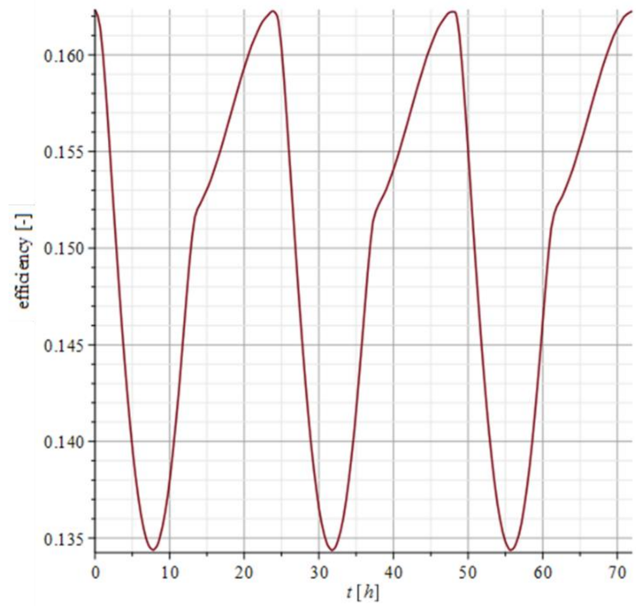

Figure 5. Variation of the PV cell efficiency over time.

The power output curve (P_{el}) over time is depicted in Figure 6. The peak power output is observed to reach 126.5 W, which occurs at t = 6.6 h after the start of the process.

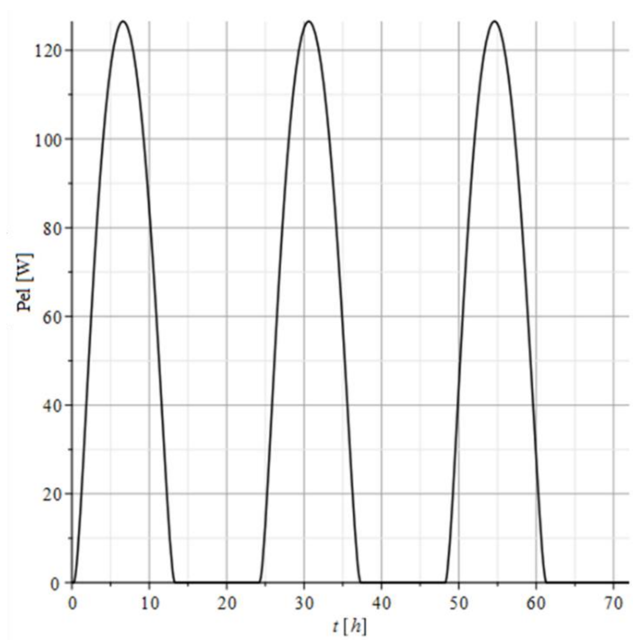

Figure 6. Time variation of the electric power output.

The convective and radiative exchange with the environment alone is insufficient for adequate heat removal from the system and cooling of the PV cell. Therefore, additional techniques are necessary to effectively reduce the PV cell temperature and improve the module efficiency. The incorporation of a PCM-containing aluminum box at the bottom of the solar panel is introduced to investigate its impact on the thermal behavior of the system, particularly the PV cell temperature and efficiency. The selection of the appropriate PCM material with suitable properties is critical as the thermal performance of the system depends on the thermophysical characteristics and thickness of the PCM. The primary objective of the optimization analysis is to determine a specific set of input parameters that minimizes the solar cell temperature.

In this analysis, our focus lies on the influential parameters of the PCM, namely the melting temperature (Tm), layer thickness (δ), and thermal conductivity (k). For the purpose of the design exploration process, we can consider the PV cell temperature as the output variable, which can be expressed as a function according to:

$$T_c = T_c\left(T_m, k, \delta\right) \tag{23}$$

Based on the findings from the design of experiments (DOE) and response surface analysis, initial estimates are provided for the input parameter values required for the subsequent optimization analysis. The goal of the optimization process is to identify a specific set of input parameters that minimizes the output variable of interest. Utilizing the parameter combinations T4-3(55,9.8,0.048) and T4-4(53,8,0.048) obtained from the optimization, the results of these cases are depicted in Fig. 7. It can be observed that in the optimized configurations, the maximum cell temperatures reach values of approximately 57°C, representing a reduction of about 20% compared to the reference case. This demonstrates that the use of a PCM with carefully selected influencing parameters based on the boundary and operational conditions can significantly extend the duration of overheating protection. Furthermore, the optimized cell efficiencies over time are presented in Fig. 8. In comparison to the reference case, the minimum efficiency values in the optimized configurations increase by 7.4% and 8.2% respectively, indicating an improvement in overall performance.

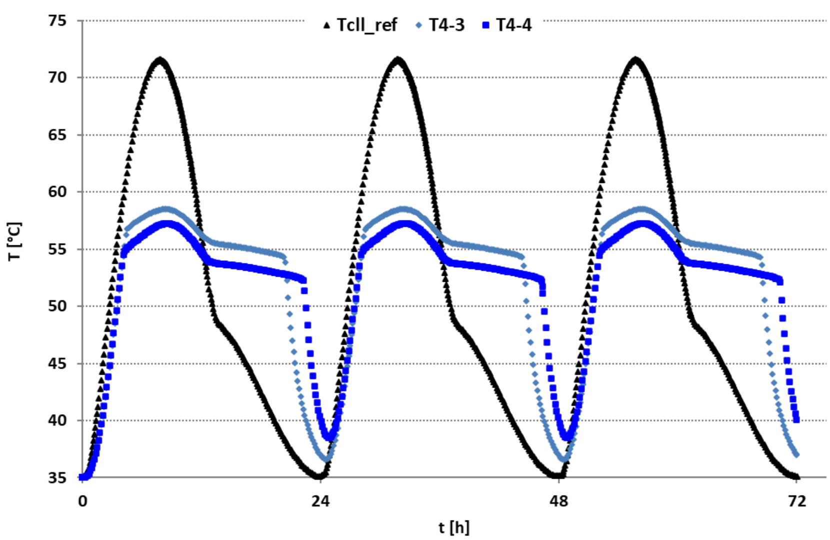

Figure 7. Evolution of PV cell temperature after optimization.

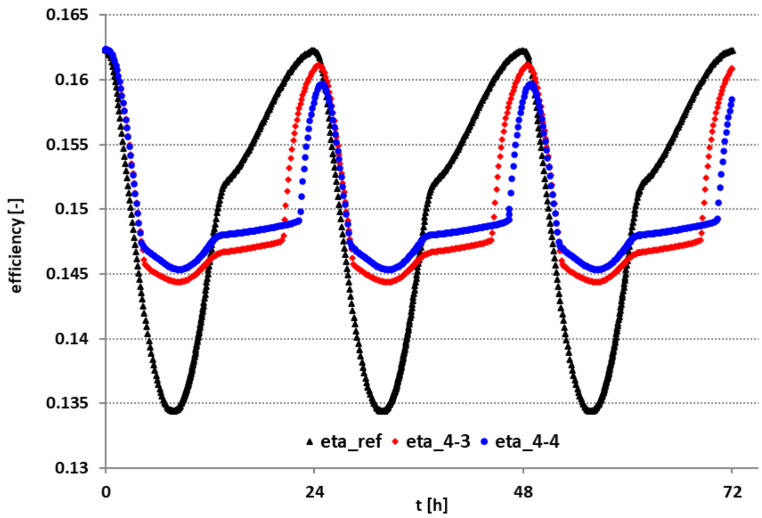

Figure 8. Optimized PV cell efficiency.

Figure 9 illustrates the comparison of electrical power output between the optimized configuration and the reference case. As a result of the improved efficiency in the optimized configuration, the maximum power output value increases by 7.8%. This highlights the significance of the optimization process in selecting input parameters that maximize the desired outputs.

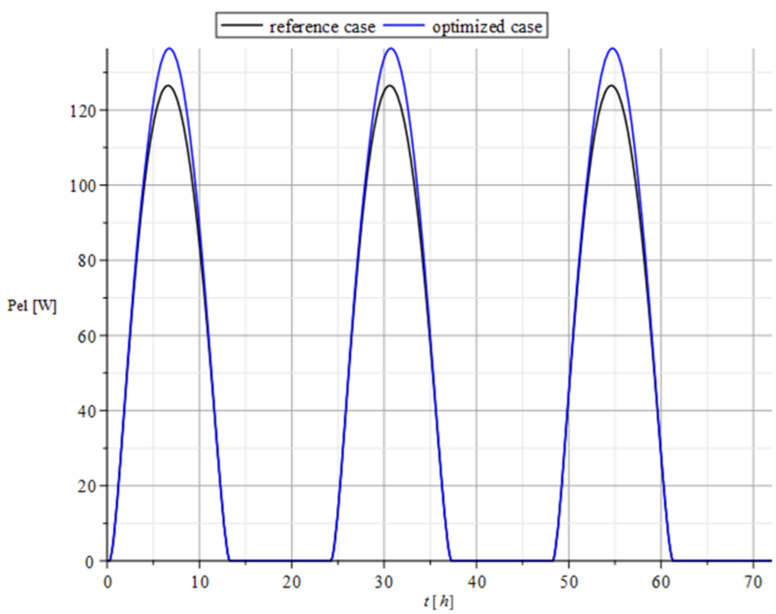

Figure 12. Optimized power output.

CONCLUSIONS

This study involves a numerical investigation of the thermal performance of a solar PV module with PCM-based thermal regulation. The focus is on analyzing the effects of material properties and thickness on the module's performance, particularly on PV cell efficiency and power output. The computational model accounts for the system's transient and nonlinear behavior, considering the time-varying solar irradiance and high ambient temperatures exceeding 50°C as key thermal boundary conditions. Selecting the most suitable PCM with the appropriate parameters is crucial but complex, as it depends on the specific thermal operating conditions. To address this challenge, an optimization analysis is conducted by integrating the thermal model with design exploration tools and employing design of experiment and response surface methodologies. This comprehensive approach enables a systematic evaluation and identification of the optimal PCM configuration for enhanced thermal performance.

REFERENCES

Alizadeh, H, R. Ghasempour, R, et al. 2018. Numerical simulation of PV cooling by using single turn pulsating heat pipe, *International Journal of Heat and Mass Transfer* 127: 203-208

Alqallaf, H.J., and Alawadhi, E.M. 2013. Concrete roof with cylindrical holes containing PCM to reduce the heat gain, *Energy and Buildings* 61: 73–80

Al-Waeli, Ali H.A., Chaichan, Miqdam T, Kazem , Hussein, Sopian, K., Ibrahim, Adnan, Mat, Sohif , Ruslan, Mohd Hafidz. 2018. Comparison study of indoor/outdoor experiments of a photovoltaic thermal PV/T system containing SiC nanofluid as a coolant. *Energy* 151: 33-44

Browne, M.C., Norton, B, and McCormack, S.J. 2015. Phase change materials for photovoltaic thermal management. *Renewable and Sustainable Energy Reviews* 47: 762-782

Huang, M., Eames, P., and Norton, B. 2004. Thermal regulation of building-integrated photovoltaics using phase change materials, *Int. J. Heat Mass Transf*. 47: 2715–2733

Khanafer, K, Al-Masri, A, and Vafai, K. 2022. Optimization of the utilization of phase change materials in planar structures to control and optimize energy flux. *International Communications in Heat and Mass Transfer* 139: 106481.

Khatib, T. and Elmenreich, W. 2016. Modeling Of Photovoltaic Systems Using Matlab, John Wiley & Sons, Inc., New Jersey,

Kuo, Chung-Feng, Liu , Jui-Min, Umar, Mega Lazuardi, Lan, Wei-Lun, Huang, Chao-Yang, and Syu, Sheng-Siang. 2019. The photovoltaic-thermal system parameter optimization design and practical verification. *Energy Conversion and Management* 180: 358-371.

Nada, A, El-Nagar, D.H., and Hussein H.M.S. 2018. Improving the thermal regulation and efficiency enhancement of PCM-Integrated PV modules using nano particles. *Energy Conversion and Management* 166: 735-743.

Shakibi, Hamid, Afzal, Sadegh, Shokri, Afshar, Sobhani, Behnam. 2022. Utilization of a phase change material with metal foam for the performance improvement of the photovoltaic cells. *Journal of Energy Storage* 51: 104466

Shaito, A., Hammoud, M, Kawtharani, F., Kawtharani, A., Reda, H. 2021. Power enhancement of a PV module using different types of phase change materials. *Energies* 14: 5195, 2021.

Smith, C.J., Forster, P. M., and Crook, R. 2014. Global analysis of photovoltaic energy output enhanced by phase change material cooling, *Applied Energy* 126: 21-28

Zarma, I., Ahmed, M., Ookawara, S. 2019. Enhancing the performance of concentrator photovoltaic systems using nanoparticle-phase change material heat sinks, *Energy Convers. Manag*.179: 229–242